BceAB-type antibiotic resistance transporters appear to act by target protection of cell wall synthesis

Carolin M Kobras[1], Hannah Piepenbreier[2], Jennifer Emenegger[3], Andre Sim[2], Georg Fritz[2,4] and Susanne Gebhard[1,*]

[1]*Department of Biology & Biochemistry, Milner Centre for Evolution, University of Bath, United Kingdom,* [2]*LOEWE Center for Synthetic Microbiology and Department of Physics, Philipps-Universität Marburg, Germany,* [3]*Department Biologie I, Ludwig-Maximilians-Universität Munich, Germany.*

[4]*Present address: School of Molecular Sciences, The University of Western Australia, Perth, Western Australia 6009, Australia.*

*For correspondence: Phone: +44 1225 386421; E-mail: s.gebhard@bath.ac.uk

Running title: Target protection of the cell wall

Keywords: ABC transport, antimicrobial peptide, lipid II cycle, *Bacillus subtilis*

ABSTRACT

Resistance against cell wall-active antimicrobial peptides in bacteria is often mediated by transporters. In low GC-content Gram-positive bacteria, a wide-spread type of such transporters are the BceAB-like systems, which frequently provide a high level of resistance against peptide antibiotics that target intermediates of the lipid II cycle of cell wall synthesis. How a transporter can offer protection from drugs that are active on the cell surface, however, has presented researchers with a conundrum. Multiple theories have been discussed, ranging from removal of the peptides from the membrane, internalisation of the drug for degradation, to removal of the cellular target rather than the drug itself. To resolve this much-debated question, we here investigated the mode of action of the transporter BceAB of *Bacillus subtilis*. We show that it does not inactivate or import its substrate antibiotic bacitracin. Moreover, we present evidence that the critical factor driving transport activity is not the drug itself, but instead the concentration of drug-target complexes in the cell. Our results, together with previously reported findings, lead us to propose that BceAB-type transporters act by transiently freeing lipid II cycle intermediates from the inhibitory grip of antimicrobial peptides, and thus provide resistance through target protection of cell wall synthesis. Target protection has so far only been reported for resistance against antibiotics with intracellular targets, such as the ribosome. However, this mechanism offers a plausible explanation for the use of transporters as resistance determinants against cell wall-active antibiotics in Gram-positive bacteria where cell wall synthesis lacks the additional protection of an outer membrane.

INTRODUCTION

The bacterial cell wall and its biosynthetic pathway, the lipid II cycle, are important targets for antibiotics, especially in Gram-positive bacteria that lack the protective layer of the outer membrane. Cell wall-targeting drugs include antimicrobial peptides (AMPs), which bind to cycle intermediates and prevent biosynthetic enzymes from carrying out the next reaction (1). It is hardly surprising that bacteria have developed a plethora of strategies to protect themselves against such antibiotic attack. Among the many known resistance mechanisms, a common strategy is the production of ATP-binding cassette (ABC) transporters that presumably remove AMPs from their site of action (2, 3). A major group of these are the BceAB-type transporters, which are found in many environmental and pathogenic species of the phylum Firmicutes (4). The eponymous and to date best-characterised system is BceAB of *Bacillus subtilis* (5). BceAB-type transporters comprise one permease (BceB) and two ATPases (BceA) (BceA, 6). The permeases consist of ten transmembrane helices and a large extracellular domain that is thought to contain the ligand binding region of the transporter (7, 8). Transporter production is regulated via a two-component regulatory system (TCS) consisting of a histidine kinase (BceS) and a response regulator (BceR) (BceR, 5, 7). A striking feature of these systems is that signalling is triggered by the activity of the transporter itself (9). Due to this flux-sensing strategy, signalling is directly proportional to transport activity, and the transporter effectively autoregulates its own production (Fig. 1A).

BceAB confers resistance against the AMPs bacitracin, mersacidin, actagardine and plectasin, of which bacitracin binds the lipid II cycle intermediate undecaprenyl pyrophosphate (UPP), while the others bind lipid II itself (5, 8). Considering the location of the AMPs' targets on the extracellular side of the cytoplasmic membrane, it is not immediately obvious how a membrane-embedded transporter can provide effective protection from these drugs. The mode of action of BceAB-type transporters has therefore been the subject of much debate (Fig. 1A). When first described, the *B. subtilis* system was named Bce for bacitracin efflux (5), although no evidence for the direction of transport was available. The assumption of export was based on the suggested self-protection

mechanism of the unrelated transporter BcrAB in the bacitracin producer *B. licheniformis* ATCC10716 (10, 11). BcrAB was thought to work as a 'hydrophobic vacuum cleaner' to remove the antibiotic from the membrane, akin to the human multidrug resistance transporter P-glycoprotein (12, 13). Later, BceAB was speculated to instead import bacitracin into the cytoplasm for subsequent degradation, again without direct experimental evidence (7). More recently, the transporter was proposed to act as a UPP flippase (14). In this scenario, BceAB would confer resistance by transporting UPP across the membrane to the cytoplasmic face, thereby removing the cellular target for bacitracin rather than transporting bacitracin itself. In the presence of bacitracin, BceAB was hypothesised to be inhibited by UPP-bacitracin complexes (UPP-BAC), which in turn should activate signalling through the BceRS two-component system to adjust BceAB levels in the cell (14). This model offered a neat explanation of the available data on bacitracin resistance, but could not explain how the same transporter can confer resistance against AMPs that target lipid II instead of UPP.

Since then, we have shown that BceB is able to bind bacitracin *in vitro* (6). Without excluding the possibility of BceAB interacting with the UPP-BAC complex, this finding suggested that BceAB-like transporters directly interacted with the AMP and that the AMP is at least part of the physiological substrate. Moreover, the computational model used to establish the flux-sensing mechanism for signalling within the Bce system was based on recognition of UPP-BAC complexes by the transporter and removal of bacitracin from the complex (9). Although the model did not specify a particular direction of transport, such a mechanism was most in line with the initial hydrophobic vacuum cleaner hypothesis (5). Resistance in this scenario is conferred by BceAB recognising target-AMP complexes in the membrane, removing the antibiotic and releasing it into the extracellular milieu. This frees the target from the inhibitory action of the antibiotic and allows the next step of cell wall synthesis to proceed.

Considering the relevance of BceAB-like systems among Firmicutes bacteria, we here set out to address the controversial question on their mode of action and how a transporter can provide effective protection against cell surface-active antibiotics. Using a peptide release assay, we exclude that BceAB acts by import or inactivation of bacitracin. Based on the discovery that signalling within the Bce system is directly proportional to transport activity, we established a promoter-reporter assay as a proxy for transport activity. Our results show that the critical variable in determining transport activity of BceAB is bacitracin in complex with its cellular target UPP, rather than bacitracin or the lipid carrier alone. Taking together the findings of this study and the literature, we conclude that BceAB-type transporters appear to transiently free their cellular target from the inhibitory grip of the AMP and provide resistance via target protection of cell wall synthesis.

METHODS

Bacterial strains and growth conditions.

All strains used in this study are given in Table 1. *E. coli* and *B. subtilis* strains were routinely grown at 37 °C with agitation (180 rpm) in lysogeny broth (LB) medium. Solid media contained 1.5% (w/v) agar. Selective media contained ampicillin (100 µg ml^{-1}), chloramphenicol (5 µg ml^{-1}), kanamycin (10 µg ml^{-1}), spectinomycin (100 µg ml^{-1}), tetracycline (10 µg ml^{-1}) or erythromycin (1 µg ml^{-1}) with lincomycin (25 µg ml^{-1}; macrolide-lincosamide-streptogramin B; mls). For full induction of the promoter P_{xylA}, xylose was added to a final concentration of 0.2 % (w/v). Bacterial growth was routinely monitored as optical density at 600 nm wavelength (OD_{600}) measured spectrophotometrically in cuvettes of 1 cm light path length.

Strain construction and molecular cloning.

All plasmids used in this study are listed in Table 1; primer sequences are given in Table 2. *B. subtilis* transformations were performed using a modified version of the Paris protocol (15). Overnight

cultures of recipient strains were grown in 500 µl Paris medium (6.1 mM K_2HPO_4, 4.4 mM KH_2PO_4, 0.4 mM trisodium citrate, 1 % (w/v) glucose, 20 mM potassium L-glutamate, 0.1 % (w/v) casamino acids, 3 mM $MgSO_4$, 25 µg ml^{-1} tryptophan, 8 µM ferric ammonium citrate) at 37 °C with aeration (180 rpm). Day cultures (500 µl) were inoculated 1:50 in fresh, pre-warmed Paris medium and grown for three hours (37 °C, 180 rpm). To each culture, 50 µl of isolated genomic DNA (gDNA) of the donor strain, or 0.5-1 µg of isolated plasmid DNA were added. Transformation cultures were grown for five more hours and plated on selective media. For mls or chloramphenicol resistance, cultures were pre-induced for one hour at 1:40 of the final concentration of the respective antibiotic. Donor strain gDNA was isolated by mixing an overnight culture of the donor 1:1 with SC buffer (150 mM NaCl, 10 mM sodium citrate, pH 7.0) and harvesting the cells by centrifugation (5 min, 1300 × *g*). The pellet was resuspended in SC buffer and incubated with lysozyme at 37 °C for 15 minutes. The solution was mixed 1:1 with 5 M NaCl and passed through a 0.45 µm syringe-driven filter. Plasmid DNA was isolated from *E. coli* using conventional mini-prep kits.

To create a construct for inducible expression of *bcrC*, the gene was PCR-amplified from *B. subtilis* W168 using primers TM2731 and TM2732, which incorporated prefix and suffix, respectively, of the modified 'Freiburg standard' of BioBrick cloning described previously (16). The resulting fragment was cloned into pSB1A3 via the EcoRI and PstI restriction sites (pJNESB101). The *bcrC* gene was then re-excised using XbaI and PstI. Assembly with an EcoRI/SpeI fragment of the BioBrick carrying the xylose-inducible promoter P_{xylA} (16) into EcoRI/PstI digested pBS2E resulted in the inducible P_{xylA}-*bcrC* construct pJNE2E01. A transcriptional P_{psdA}-*lux* reporter construct (pSDlux102) was created by PCR amplification of the promoter region of *psdAB* of *B. subtilis* using primers TM0599 and TM2242, and ligation with pAH328 via EcoRI and NotI restriction sites. The existing P_{bceA}-*luxABCDE* reporter (pSDlux101; (17) was re-constructed in vector pBS3Elux (18), which contains an mls resistance marker instead of chloramphenicol. This was achieved by PCR amplification of the promoter fragment with primers SG843 and SG883, and cloning via EcoRI and PstI sites, resulting in plasmid pMG3Elux1.

Determination of the minimal inhibitory concentration

The susceptibility of *B. subtilis* strains to bacitracin was determined using the minimal inhibitory concentration (MIC) determined by broth micro-dilutions. For this, two-fold serial dilutions of Zn^{2+}-bacitracin were prepared in 2 ml of Mueller-Hinton medium and inoculated 1:500 from overnight cultures grown in the same medium. For higher resolution, in some instances defined concentrations of Zn^{2+}- bacitracin were added directly to each culture. Cultures were incubated overnight (37 °C, 180 rpm) and examined for growth after 24 h. The MIC was determined as the lowest concentration at which no visible growth was detected. All experiments were performed in at least biological triplicates, and mean values and standard deviations were calculated to report the data.

Bacitracin uptake assays

Bacitracin uptake was assayed with slight modification to previously described protocols (19, 20). Overnight cultures were diluted 1:500 in 100 ml LB supplemented with 1 % (w/v) fructose. To induce BceAB production in the wild type, 1 µg ml^{-1} bacitracin was added at the time of inoculation. The cultures were incubated for 3.5-4.75 h at 37 °C (200 rpm) until they reached an OD_{600} of 1.0-2.0. Cells were harvested by centrifugation (4000 × *g*, 10 minutes, room temperature) and washed twice with 50 mM potassium phosphate (pH 7-7.5) and 100 mM NaCl. Cell density was adjusted to an OD_{600} of 10 in assay buffer (50 mM potassium phosphate (pH 7-7.5), 100 mM NaCl, 1 % (w/v) fructose and 50 µM zinc sulfate). Aliquots of 2.4 ml of the cell suspension were incubated for 10 minutes at 37°C (200 rpm). Bacitracin was added to a final concentration of 5 µg ml^{-1}, followed by incubation for 30 minutes at 37 °C (200 rpm). As control, one sample containing no cells received the identical treatment. Cells were removed by centrifugation (4000 × *g*, 10 minutes, room temperature) and the supernatants were filtered (0.45 µm). The supernatants were stored for no longer than five days at -

20 °C, and were concentrated 5-fold using an Eppendorf Concentrator 5301 speed vacuum at room temperature.

To quantify the bacitracin remaining in the culture supernatants, the sensitivity of the strain TMB713 was exploited in a bioassay adapted from the method established by K. Okuda et al. (21). To this end, an overnight culture of TMB713, grown in LB with selective antibiotics, was diluted 1:30 into 3 ml melted (60 °C) LB soft agar (0.75 % (w/v)) and poured evenly onto a dried LB agar plate, allowed to solidify 10 minutes at room temperature and then dried for 10 minutes. Plugs 6 mm in diameter were removed from the plate, leaving stable holes in the agar. In volumes of 50 µl, bacitracin standards (5-50 µg ml^{-1}) and concentrated supernatants were applied into the holes and plates were immediately incubated upright at 37°C. After 24-26 hours, the diameter of the growth inhibition zone was measured. Clearing zones measured from bacitracin standards were used to create a standard curve. Bacitracin concentrations in supernatants were extrapolated using the standard curve and worked back to the original sample from the known 5-fold concentration factor during sample preparation.

Computational model and simulations

Model predictions for the data in figures 3 and 4 were performed with a previously established model for the lipid II cycle and its interaction with the bacitracin stress response network in *B. subtilis* (22, 23). Briefly, the model uses deterministic differential equations to describe the time-dependent concentrations of the different lipid II cycle intermediates, as well as the bacitracin stress response modules BcrC and BceAB. A detailed description of the model assumptions and equations for the bacitracin resistance network in *B. subtilis* wild type and the Δ*bcrC* mutant has been laid out before (23). In the model for the Δ*bcrC* mutant, a homeostatic up-shift in *de novo* synthesis of UPP leads to maintenance of PG synthesis to ensure *bcrC* deletion is not lethal (23). This additional increase in carrier pool exacerbates the accumulation of UPP even further. To illustrate the model

189 behavior for a *bcrC* overexpression strain (Fig. 4B), we assumed that this strain features a 1.5-fold
190 stronger UPP phosphatase activity compared to wild-type cells, based on the higher activity of the
191 P_{xylA} promoter driving *bcrC* expression in this strain (9) relative to the native P_{bcrC} promoter (24). All
192 numerical simulations of the differential equations were performed with custom scripts developed
193 in MATLAB™ software (The MathWorks, Inc.).

194

195 **Luciferase reporter assay**

196 For reporter gene assays, 10 ml of LB or modified chemically defined medium (MCSE, as described in
197 16) were inoculated 1:1000 from overnight cultures of each strain to be tested. Day cultures were
198 grown at 37 °C with agitation (180 rpm) to an OD_{600} of around 0.5, to ensure exponential growth.
199 Cultures were then diluted into fresh growth medium to an OD_{600} of 0.01 and distributed into 96
200 well microplates (Corning®, black, clear flat bottom), with 100 µl culture volume per well. Wells
201 around the plate edge were filled with water to reduce evaporation. Luciferase activity of strains was
202 determined in a Tecan® Spark® microplate reader controlled by the SparkControl™ software (Tecan
203 Trading AG, Switzerland). Cells were grown in the microplate reader for 5 hours with continuous
204 shaking incubation (37 °C, 180 rpm, orbital motion, amplitude: 3 mm). After one hour of incubation,
205 cells were challenged with varying concentrations of antibiotic. The OD_{600} and luminescence (relative
206 luminescence units, RLU) were measured every 5 minutes (integration time: 1000 ms).
207 Luminescence output was normalized to cell density by dividing each data point by its corresponding
208 blank-corrected OD_{600} value (RLU OD^{-1}). For dose response curves, RLU OD^{-1} values were determined
209 from the average of three data points taken at steady-state (25, 30 and 35 min). Experiments were
210 carried out at least in biological triplicates. To determine the dose response behaviour of strains for
211 bacitracin, luminescence values were normalised, with 0 % defined as the lowest, and 100 % as the
212 highest measured RLU OD^{-1} value for each strain. Data were then fitted with variable slope dose-
213 response curves in GraphPad Prism7, using the logarithms of bacitracin concentrations as x, and

214 normalised luminescence as y values, and applying default settings. Statistical comparison of the

215 resulting EC_{50} values was performed using the in-built comparison tool for non-linear regression fits

216 of GraphPad Prism 7, based on an extra sum-of-squares F test.

RESULTS AND DISCUSSION

BceAB does not import or inactivate bacitracin.

To investigate the resistance mechanism of BceAB-type transporters, we first focussed on the direction of transport by BceAB. To this end, we applied a modified version of the peptide release assay established by Otto and colleagues (19). This is based on quantification of the AMP concentration that remains in the culture supernatant after incubating cell suspensions of bacteria carrying or lacking the transporter in an AMP-containing buffer. Presence of an importer should lead to a decrease in the AMP concentration remaining in the buffer, while an increase in AMP concentration compared to transporter-negative cells would be indicative of a mechanism where the drug is expelled from the bacterial cell envelope (19, 20). To quantify the remaining bacitracin, we chose a bioassay-based method, similar to the technique reported by Okuda and colleagues (21, see methods for details) . This would allow us to determine the amount of biologically active peptide remaining, to provide additional information on whether the action of BceAB may somehow inactivate the antibiotic.

Earlier models for BceAB action considered bacitracin import, potentially followed by intracellular degradation (7). Alternative conceivable mechanisms of resistance could be inactivation of the extracellular AMP, e.g. through shedding of phospholipids, which could be catalysed by BceAB, akin to a mechanism reported for daptomycin resistance in *S. aureus* (25). However, our bio-assay methodology did not show any significant reduction in bacitracin activity by BceAB-containing cells (i.e. wild-type cells that had been pre-induced with low concentrations of bacitracin to ensure *bceAB* expression), arguing against such mechanisms (Fig. 2). We observed a slight reduction in active bacitracin compared to the starting concentration of 5 µg ml^{-1}, but this applied to all samples, including the buffer-control. Therefore, it was likely due to the known oxidative deamination of bacitracin A to bacitracin F, which lowers the antimicrobial activity (26), during incubation and

241 sample processing. Our data thus indicate that BceAB neither imports bacitracin into the cell, nor
242 inactivates or degrades bacitracin in the extracellular space.

243 When we compared BceAB positive and negative cells, we could not detect significant differences in
244 supernatant concentrations of the drug (Fig. 2). This was not in line with our hypothesis that BceAB
245 should expel bacitracin from the membrane into the extracellular milieu. In a recent study on the
246 BceAB-type transporter NsrFP from *Streptococcus agalactiae* COH1, which used a similar peptide
247 release assay, the residual AMP concentration in the culture supernatant was significantly higher in
248 an *nsrFP*$^{+}$ strain compared to strains with no or inactive NsrFP, in agreement with a 'hydrophobic
249 vacuum cleaner' mechanism as proposed for BceAB (27). The main difference to our study was that
250 the NsrFP experiments were done using the lantibiotic nisin as substrate, and earlier similar studies
251 had also used lantibiotic substrates (19, 20, 28). As lantibiotics and bacitracin have fundamentally
252 different modes-of-action, we believe that the peptide release assay may not have been sensitive
253 enough to detect small differences in the amount of bacitracin attached to the cells.

254 Nevertheless, based on the homology between BceAB and NsrFP, it is plausible that both employ the
255 same functional mechanism (27). Further support for the expulsion of AMPs from the membrane is
256 provided by the LanFEG-type transporters, which use such a strategy to confer self-immunity in
257 AMP-producing bacteria. Well-known examples of this group include the transporters NisFEG of
258 *Lactococcus lactis* and SpaFEG of *B. subtilis* (2). Several studies have shown that these transporters
259 effectively mediate resistance against AMPs without degrading or inactivating the drugs, but by
260 releasing them into the culture supernatant (19, 20, 28, 29). Although LanFEG transporters share no
261 close evolutionary relationship with BceAB-type systems (2), the fact that they impart resistance
262 against the same range of antibiotics lends weight to the hypothesis that both use a similar principle
263 of protection.

264 BceAB-type systems belong to the Type VII ABC transporter superfamily, of which the *E. coli*
265 macrolide resistance transporter MacB is the paradigm example (30). MacB was recently shown to

act according to a molecular bellows mechanism and expel its substrate from the periplasm across the outer membrane via the TolC exit duct by undergoing extensive conformational changes in its periplasmic domain (31). This mode of 'transport', which does not involve physical movement of a substrate across a membrane but instead uses intracellular ATP hydrolysis to perform mechanical work in the periplasm, was termed 'mechanotransmission' (31). BceAB shares the critical features of MacB that are required for the mechanotransmission mechanism (30). In this case, the work carried out by the transporter would be to shift the equilibrium of the bacitracin binding reaction from the membrane more towards the extracellular environment. For such a 'hydrophobic vacuum cleaner' mechanism to work, the transporter will need to distinguish between the membrane-bound and the free form of the AMP. Interestingly, bacitracin undergoes an extensive conformational change upon binding its cellular target, from a free state with no clear hydrophobic moment, to an amphipathic, closed dome-shaped conformation when bound to UPP (32). While we have shown previously that BceAB was able to bind bacitracin *in vitro*, these experiments were carried out with detergent-solubilised protein that may have contained co-purified membrane lipids (6). We therefore cannot draw any direct conclusions on whether it interacted with the free drug, or with any bacitracin-UPP complexes (UPP-BAC) that may have been present in the experiment. Therefore, we next aimed to identify the physiological substrate of BceAB *in vivo.*

Exploiting the flux-sensing mechanism as suitable strategy to monitor BceAB activity.

To study the function of BceAB *in vivo*, we first required a strategy to quantify transport activity in living cells. We previously showed that signalling within the Bce system is directly proportional to BceAB transport activity (9). As the signalling cascade ultimately leads to activation of the promoter controlling *bceAB* expression (P_{bceA}), the activity of a P_{bceA}-*luxABCDE* reporter fusion can therefore be taken as a proxy for BceAB activity (Fig. 1A). Using this approach, we monitored BceAB activity in the wild-type strain carrying the reporter fusion (SGB73, WT) under several sub-inhibitory bacitracin concentrations. In agreement with earlier data (9), the threshold concentration to elicit detectable BceAB activity was 0.03 µg ml^{-1} bacitracin, and the activity gradually increased until maximum levels

292 were reached at 30 µg ml^{-1} (Fig. 1B). As it was previously shown that higher bacitracin
293 concentrations did not cause a further increase in activity (7, 9, 24), we deemed this concentration a
294 suitable endpoint.

295

296 **Accumulation of UPP specifically increases BceAB activity at low bacitracin concentrations.**
297 While the preliminary experiment in Fig. 1B showed that transport activity increased with higher
298 bacitracin concentrations, it did not allow us to distinguish between free bacitracin and UPP-BAC as
299 substrates. This is because the concentration of UPP-BAC will change proportionally to the
300 concentration of bacitracin added to the culture (Fig. 1C). To distinguish whether the critical variable
301 determining BceAB transport activity was bacitracin itself or the UPP-BAC complex, we required a
302 strategy to change the concentration of UPP-BAC, while keeping the concentration of bacitracin
303 constant. Considering the reaction equilibrium between bacitracin and UPP-BAC (Fig. 1C), this should
304 be possible by adjusting the cellular levels of UPP, as increased amounts of UPP result in higher
305 concentrations of UPP-BAC without altering the bacitracin concentration.

306 To find a suitable genetic approach to change the UPP levels in the cell, we turned to mathematical
307 modelling. Based on the computational description of the lipid II cycle (22), we recently developed a
308 mathematic model that describes the protective effect of the bacitracin resistance determinants
309 BceAB and BcrC of *B. subtilis* on the progression of the lipid II cycle (23). This model can predict
310 changes to the pool levels of lipid II cycle intermediates under different conditions and suggests that
311 reducing the rate of UPP dephosphorylation increases the level of UPP displayed on the extracellular
312 face of the membrane. In *B. subtilis*, the dephosphorylation reaction of UPP to UP is catalysed by
313 two phosphatases, BcrC and UppP (33-35). BcrC plays the more prominent role during exponential
314 growth, and *bcrC* deletion should thus have the bigger effect on reducing the rate of
315 dephosphorylation. In a Δ*bcrC* scenario, the model predicted the UPP pool to increase more than
316 eight-fold over the wild-type levels (Fig. 3A&B).

To exploit this finding, we deleted *bcrC* in our reporter strain (Δ*bcrC*). When we re-tested this strain for BceAB activity, we observed a striking 10-fold reduction in the threshold concentration required to trigger detectable transport activity (0.003 µg ml^{-1}, Fig. 3C). Likewise, maximum BceAB activity was observed at 0.3 µg ml^{-1} bacitracin (Fig. 3C, turquoise), 100-fold less than required to reach a similar activity in the wild type (Fig. 3C, dark blue). Fitting of a dose-response curve to the normalised data for both strains (see methods for details) showed that indeed the half-maximal effective concentration of bacitracin (EC_{50}), i.e. the concentration where BceAB activity was half its maximum, was shifted from 5.5 µg ml^{-1} in the wild type to 0.05 µg ml^{-1} in the Δ*bcrC* strain (Fig. S1A). Importantly, the overall shape of the curve was not altered between strains, showing that the differences were solely due to changes in substrate concentration upon UPP accumulation, not any mechanistic changes in the transporter itself that may have been caused by *bcrC* deletion. To explore if UPP alone could serve as the physiological substrate of BceAB, the activity was also compared in the absence of bacitracin. There was no detectable BceAB activity in either of the tested strains, which suggested that accumulation of UPP alone was not sufficient to trigger transport by BceAB. These findings were a first indication that the critical variable that determines BceAB activity is the concentration of UPP-BAC complexes, rather than bacitracin or UPP alone.

In the wild type, induction of P_{bceA} of course not only drives reporter gene expression but also increases the amount of BceAB present in the cell. To exclude that the observed sensitivity shift upon UPP accumulation was not due to changes in *bceAB* expression, we uncoupled BceAB production from its native regulation. This was achieved by deleting the native copy of *bceAB* in the reporter strain and introducing an ectopic copy under xylose-inducible control (P_{xylA}-*bceAB*; strain SGB218). The same was done in the Δ*bcrC* reporter, resulting in strain SGB677. Comparing BceAB activity in these two strains again showed a marked decrease (30-fold) in the threshold bacitracin concentration required to trigger detectable activity upon accumulation of UPP (Fig. S1B). This shows that the observed shift in sensitivity of BceAB could not be explained by indirect regulatory effects on *bceAB* expression.

343 Accumulation of UPP may have caused wider alterations in the cell membrane and/or affected
344 BceAB activity in a non-specific manner, rather than the intended change in the concentration of
345 UPP-BAC complexes. Therefore, we next tested if *bcrC* deletion also altered BceAB activity in
346 response to AMPs that do not interfere with UPP. To this end, we measured BceAB activity in
347 response to mersacidin and deoxy-actagardine B, two other AMPs that are known substrates for
348 BceAB (8). As both of these peptides target lipid II but not UPP, the complex formation between
349 these AMPs and their respective cellular target should be unaffected by changes in the UPP level.
350 Indeed, our theoretical model predicted that the lipid II pool on the extracellular face of the
351 membrane would remain almost unchanged in a Δ*bcrC* scenario compared to the wild type (Fig.
352 3A&B). This is because the total amount of lipid carrier is homeostatically increased in a *bcrC*
353 deletion strain to ensure a close-to-optimal rate of peptidoglycan synthesis (23). The model
354 therefore confirms that decreasing the UPP dephosphorylation rate in the Δ*bcrC* strain specifically
355 causes accumulation of UPP but does not affect other cycle intermediates.

356 As with bacitracin, a gradual increase of BceAB activity was observed with increasing amounts of
357 mersacidin or deoxy-actagardine B, in both the wild type and Δ*bcrC* strains (Fig. 3D, E). However, we
358 did not observe any significant differences in threshold substrate concentrations nor overall BceAB
359 activity between the two strains. As an additional control, we tested the activity of a second BceAB-
360 type transporter in *B. subtilis*, PsdAB, which confers resistance against nisin, another lipid II binding
361 AMP (8). PsdAB activity was determined using the same luminescence-based assay principle as for
362 BceAB, but with P_{psdA} activity as a proxy for transport activity. As before, activity increased with nisin
363 concentration in both the wild type and Δ*bcrC* mutant, but again no significant differences between
364 strains were observed (Fig. 3F). These findings show that *bcrC* deletion and concomitant
365 accumulation of UPP did not have a general effect on BceAB or PsdAB function. Instead, BceAB
366 activity appeared to specifically depend on the concentration of UPP-BAC in the membrane. This is
367 consistent with the proposed hypothesis for a 'hydrophobic vacuum cleaner' mechanism of

transport, suggesting that the physiological substrate of BceAB is indeed the antibiotic in complex with its cellular target.

Depletion of UPP affects transport activity on a global level

To further explore the effect of altered UPP levels on BceAB activity, we next sought to decrease the pool of UPP displayed on the outer face of the membrane, and hence the amount of UPP-BAC complexes formed. The mathematical model predicted that an increased rate of UPP dephosphorylation, e.g. by overproducing BcrC, may lead to such a decreased UPP pool (Fig. 4A&B), although differences to the wild type are less pronounced than with *bcrC* deletion. To realise this experimentally, we overproduced BcrC by placing an additional copy of *bcrC* under control of the xylose-inducible promoter P_{xylA} (SGB758). Testing the BceAB activities in the strain with reduced UPP levels led to overall lower activity upon addition of bacitracin, and even at the maximal concentration tested the activity was less than 50 % of the wild-type activity (Fig. 4C). The threshold concentration required to trigger detectable activity was only marginally increased. Fitting the normalised activities with a dose-response curve produced identical results for both strains (Fig. S1C). This suggests that BcrC overproduction led to an overall decrease in BceAB activity, but had no effect on the transporter's sensitivity to the substrate. Also consistent with a more global effect of BcrC overproduction on cell physiology, was the observation that BceAB activity was similarly reduced when mersacidin and deoxy-actagardine B were tested (Fig. 4D&E). Likewise, the activity of PsdAB using nisin as substrate was also reduced (Fig. 4F). It therefore appears that overproduction of BcrC did not have the desired effect of solely reducing the UPP pool in the cell, but instead led to wider-ranging changes that affected either multiple stages of the lipid II cycle, explaining similar effects on bacitracin and lipid II-binding AMPs, or impeded the mechanical functions of the membrane-embedded transporters to reduce their overall activity. Without further knowledge on the precise cellular effects of BcrC overproduction it is difficult to interpret these results. However,

393 while they do not further support our hypothesis that BceAB recognises its substrate AMP as a
394 complex with the cellular target, they also do not disprove it.

395

396 **Accumulation of C_{35}-PP (HPP) does not inhibit BceAB activity.**

397 In addition to the theories on bacitracin import, export or inactivation by BceAB-type transporters, a
398 drastically different mechanism has been proposed where BceAB could protect the cell from
399 bacitracin by flipping UPP from the outer leaflet of the membrane to the inner face, thereby
400 shielding it from the AMP (14). This hypothesis was based on the observation that accumulation of
401 the C_{35} isoprenoid heptaprenyl diphosphate (HPP) in the membrane sensitises the cell to bacitracin.
402 HPP was hypothesised to act as a competitive inhibitor of BceAB and to reduce its transport activity
403 (14). To explore this hypothesis further, we next tested the effect of HPP accumulation on BceAB
404 activity, using the luciferase-based assay described above. Accumulation of HPP can be created by
405 manipulations of the isoprenoid biosynthesis pathway (14), specifically via deletion of *ytpB*, which
406 encodes a tetraprenyl-beta-curcumene synthase (Sato *et al.*, 2011), and simultaneous limitation of
407 the activity of MenA, a key enzyme in the menaquinone pathway (Kingston *et al.*, 2014). The *menA*
408 gene is essential, but a reduction in enzymatic activity can be achieved by growth in tryptophan-
409 limited conditions (14). Therefore, to determine whether BceAB activity is inhibited by HPP
410 accumulation, we tested BceAB activity in a Δ*ytpB* Δ*menA* deletion strain that carried an ectopic
411 IPTG-inducible copy of *menA* (SGB929, based on HB13438 (14)) and was grown in a tryptophan-
412 limited defined medium without addition of IPTG.
413 Interestingly, the threshold bacitracin concentration required to trigger transport, as well as the
414 activity at peak stimulation were indistinguishable between the two strains, showing that HPP
415 accumulation did not affect BceAB activity (Fig. 5). To confirm that our strategy had led to the
416 desired HPP accumulation, we tested the bacitracin sensitivity of both strains. The MIC decreased
417 from 173±12 µg ml^{-1} in the wild type to 120 µg ml^{-1} in the mutant strain, in line with the previously

418 reported increased susceptibility upon HPP accumulation (14). Based on these results, we concluded
419 that the increased bacitracin sensitivity was not due to direct inhibition of BceAB activity by HPP.
420 Instead, our interpretation is that BceAB likely cannot distinguish between UPP-BAC and HPP-BAC.
421 Bacitracin was shown to tightly interact with the pyrophosphate group and only the first isoprenoid
422 unit of its substrate, based on its co-crystal structure with the C_{10} isoprenoid geranyl pyrophosphate
423 (32). It is therefore expected that HPP will also serve as a bacitracin target in the cell, and its
424 accumulation will lead to the simultaneous presence of both UPP-BAC and HPP-BAC complexes. In
425 the context of our findings above that UPP-BAC – and by analogy also HPP-BAC – is the likely
426 physiological substrate of BceAB, it is plausible that either complex will drive BceAB activity. Hence,
427 accumulation of HPP did not affect the net transport activity. However, HPP cannot substitute for
428 UPP in the lipid II cycle. Any activity of BceAB invested in the removal of bacitracin from HPP is
429 therefore futile with respect to resistance, which can explain the increased bacitracin sensitivity
430 observed upon HPP accumulation. Taking together our findings with the previous detailed study of
431 the effects of HPP accumulation on bacitracin resistance (14), a model where BceAB removes
432 bacitracin from its cellular targets appears more in line with the available experimental evidence
433 than a UPP-flipping mechanism. Furthermore, as mentioned, BceAB also confers resistance against
434 lipid II-binding AMPs, namely mersacidin, actagardine and the fungal defensin plectasin (8, 36). For
435 these compounds, it is difficult to envisage a flipping mechanism as an effective strategy to shield
436 the target from AMP access, because import of lipid II runs counter the process of cell wall
437 biosynthesis, where peptidoglycan precursors are required on the surface of the membrane.
438

439 **CONCLUDING REMARKS.**

440 In this study, we set out to address the much-debated question on the mode-of-action of BceAB-
441 type resistance systems and how a transporter may be used to protect the cell from antibiotics that
442 have targets on the cell surface. The balance of evidence presented here and in the literature
443 appears to be in clear favour of BceAB acting as a 'hydrophobic vacuum cleaner', which is in line with

444 the mechanotransmission mechanism proposed for Type VII superfamily ABC systems (30, 31). In
445 this model, BceAB specifically recognises its substrate AMPs in complex with their respective cellular
446 target, here experimentally tested for UPP-BAC. ATP hydrolysis in the cytoplasm then provides the
447 required energy to break the interaction between bacitracin and UPP on the cell surface. This is not
448 a novel concept in a transporter, because the human cholesterol transporter ABCG5/8 employs a
449 similar mechanism to remove cholesterol from the cytoplasmic membrane of hepatocytes, using the
450 energy from ATP-hydrolysis to break the interactions between cholesterol and membrane
451 phospholipids (37). In the case of BceAB, a shift in equilibrium from target-bound AMP to free AMP
452 can be achieved if the transporter has a low affinity to the free antibiotic and therefore releases it as
453 soon as it is removed from the target. Given the substantial conformational change of bacitracin and
454 other peptides between the free and target-bound forms (1, 38-40), this seems entirely plausible. In
455 support of this idea, we have only been able to show binding of bacitracin by the entire detergent-
456 solubilised transporter, where UPP may have been co-purified (6), but never with its isolated
457 extracellular domain that provides substrate specificity in BceAB-like systems (41) and therefore is
458 thought to contain the ligand binding site (own unpublished data).

459 How then does a simple shift in equilibrium confer the high level of resistance that is the hallmark of
460 BceAB-like transporters? For one, there is ample evidence that the LanFEG-type transporters of AMP
461 producing bacteria work by exactly such a mechanism to provide effective protection from the self-
462 produced AMP (19, 20, 28, 29). Moreover, a similar principle, albeit not on the cell surface, is seen in
463 resistance against tetracyclines, a group of antibiotics that target the bacterial ribosome. Here,
464 ribosomal protection proteins like Tet(O) and Tet(M) were shown to actively release tetracycline
465 from the ribosome in a GTP-driven manner (42, 43). This mechanism effectively increases the
466 dissociation rate of tetracycline and secures continued protein synthesis (44). Interestingly, another
467 resistance system that protects ribosomal function from antibiotic attack is a group of proteins
468 referred to as Antibiotic Resistance ATP-Binding Cassette-F (ARE ABC-F). While originally annotated
469 as transporters, these proteins lack any transmembrane segments and instead act by modulating the

binding affinity between antibiotics and the ribosome, thus effectively dislodging the drugs (45, 46). This mode of resistance has been collectively termed 'target protection', and generally involves the direct release of a cellular target from the inhibitory action of the antibiotic (46, 47). Target protection has been reported for the ribosome and DNA replication (48-50), but to our knowledge no example has been described to date for protection of cell wall synthesis. We now propose that BceAB-type transporters act by target protection of the lipid II cycle. By physically freeing UPP from the grip of bacitracin (or analogously, freeing lipid II from lantibiotics), BceAB ensures that the affected enzyme (UPP-phosphatase or PG transglycosylases, respectively) can catalyse the following step of cell wall synthesis, enabling the cycle to continue at least for one more round before the antibiotic can re-bind its target. Importantly, to our knowledge this mode of action is in agreement with all experimental data currently available on BceAB-like systems. Recognition of target-AMP complexes – rather than the free peptides – offers an explanation for the seemingly random substrate specificity of BceAB-like systems (8, 51), where the specificity determinant likely only becomes apparent in the antibiotic-target complex. It also explains the observations on reduced resistance upon over-production of HPP in the cell, where some of BceAB's transport activity is likely invested in the futile removal of bacitracin from HPP rather than UPP (14). And it is consistent with the data reported here and previously (9, 23) that the factor determining transport activity of BceAB is the concentration of UPP-BAC complexes in the cell. Target protection of cell wall synthesis also offers a plausible explanation for the use of transporters in resistance against cell wall-active antibiotics in Gram-positive bacteria. Whereas the outer membrane of Gram-negative microorganisms creates a discrete compartment, and transporters can be used to change a compound's concentration in this space, Gram-positive bacteria lack an equivalent structure. It will be interesting to explore if other transport systems in these bacteria operate by a similar mechanism to protect the cell wall synthesis machinery from antibiotic attack.

ACKNOWLEDGEMENTS

The authors would like to thank John Helmann for kindly giving us strain HB13438 and its progenitors, and Cantab Anti-Infectives Ltd. for the generous gift of mersacidin and deoxy-actagardine B. We also thank Marjorie Gibbon and Sebastian Dintner for cloning of luciferase reporter constructs.

Work in SG's lab was supported by the Biotechnology and Biological Sciences Research Council (BBSRC; BB/M029255/1). CMK was supported by a University of Bath Research Studentship Award. Work in GF's group was supported by the LOEWE Program of the State of Hesse (SYNMIKRO) and the Deutsche Forschungsgemeinschaft (DFG; FR3673/1-2). HP was supported by the Cusanuswerk scholarship program (Germany).

JE's contributions were the results of a master's research project carried out at LMU Munich in 2013 under supervision of SG and GF.

REFERENCES

1. Breukink E, de Kruijff B. 2006. Lipid II as a target for antibiotics. Nat Rev Drug Discov 5:321-32.
2. Gebhard S. 2012. ABC transporters of antimicrobial peptides in Firmicutes bacteria - phylogeny, function and regulation. Mol Microbiol 86:1295-317.
3. Revilla-Guarinos A, Gebhard S, Mascher T, Zuniga M. 2014. Defence against antimicrobial peptides: different strategies in Firmicutes. Environ Microbiol 16:1225-37.
4. Dintner S, Staron A, Berchtold E, Petri T, Mascher T, Gebhard S. 2011. Coevolution of ABC transporters and two-component regulatory systems as resistance modules against antimicrobial peptides in Firmicutes Bacteria. J Bacteriol 193:3851-62.
5. Ohki R, Giyanto, Tateno K, Masuyama W, Moriya S, Kobayashi K, Ogasawara N. 2003. The BceRS two-component regulatory system induces expression of the bacitracin transporter, BceAB, in *Bacillus subtilis*. Mol Microbiol 49:1135-1144.
6. Dintner S, Heermann R, Fang C, Jung K, Gebhard S. 2014. A sensory complex consisting of an ATP-binding cassette transporter and a two-component regulatory system controls bacitracin resistance in *Bacillus subtilis*. J Biol Chem 289:27899-910.
7. Rietkötter E, Hoyer D, Mascher T. 2008. Bacitracin sensing in *Bacillus subtilis*. Mol Microbiol 68:768-85.
8. Staron A, Finkeisen DE, Mascher T. 2011. Peptide antibiotic sensing and detoxification modules of *Bacillus subtilis*. Antimicrob Agents Chemother 55:515-25.

9. Fritz G, Dintner S, Treichel NS, Radeck J, Gerland U, Mascher T, Gebhard S. 2015. A New Way of Sensing: Need-Based Activation of Antibiotic Resistance by a Flux-Sensing Mechanism. MBio 6:e00975.
10. Podlesek Z, Comino A, Herzog-Velikonja B, Zgur-Bertok D, Komel R, Grabnar M. 1995. *Bacillus licheniformis* bacitracin-resistance ABC transporter: relationship to mammalian multidrug resistance. Mol Microbiol 16:969-76.
11. Podlesek Z, Comino A, Herzog-Velikonja B, Grabnar M. 2000. The role of the bacitracin ABC transporter in bacitracin resistance and collateral detergent sensitivity. FEMS Microbiol Lett 188:103-6.
12. Higgins CF, Gottesman MM. 1992. Is the Multidrug Transporter a Flippase. Trends in Biochemical Sciences 17:18-21.
13. Gottesman MM, Pastan I. 1993. Biochemistry of multidrug resistance mediated by the multidrug transporter. Annu Rev Biochem 62:385-427.
14. Kingston AW, Zhao H, Cook GM, Helmann JD. 2014. Accumulation of heptaprenyl diphosphate sensitizes *Bacillus subtilis* to bacitracin: implications for the mechanism of resistance mediated by the BceAB transporter. Mol Microbiol 93:37-49.
15. Kunst F, Rapoport G. 1995. Salt stress is an environmental signal affecting degradative enzyme synthesis in *Bacillus subtilis*. J Bacteriol 177:2403-7.
16. Radeck J, Kraft K, Bartels J, Cikovic T, Dürr F, Emenegger J, Kelterborn S, Sauer C, Fritz G, Gebhard S, Mascher T. 2013. The *Bacillus* BioBrick Box: generation and evaluation of essential genetic building blocks for standardized work with *Bacillus subtilis*. J Biol Eng 7:29.
17. Kallenberg F, Dintner S, Schmitz R, Gebhard S. 2013. Identification of regions important for resistance and signalling within the antimicrobial peptide transporter BceAB of *Bacillus subtilis*. J Bacteriol 195:3287-97.
18. Popp PF, Dotzler M, Radeck J, Bartels J, Mascher T. 2017. The *Bacillus* BioBrick Box 2.0: expanding the genetic toolbox for the standardized work with *Bacillus subtilis*. Sci Rep 7:15058.
19. Otto M, Peschel A, Gotz F. 1998. Producer self-protection against the lantibiotic epidermin by the ABC transporter EpiFEG of *Staphylococcus epidermidis* Tu3298. FEMS Microbiol Lett 166:203-11.
20. Stein T, Heinzmann S, Solovieva I, Entian KD. 2003. Function of *Lactococcus lactis* nisin immunity genes *nisI* and *nisFEG* after coordinated expression in the surrogate host *Bacillus subtilis*. J Biol Chem 278:89-94.
21. Okuda K, Yanagihara S, Sugayama T, Zendo T, Nakayama J, Sonomoto K. 2010. Functional significance of the E loop, a novel motif conserved in the lantibiotic immunity ATP-binding cassette transport systems. J Bacteriol 192:2801-8.
22. Piepenbreier H, Diehl A, Fritz G. 2019. Minimal exposure of lipid II cycle intermediates triggers cell wall antibiotic resistance. Nat Commun 10:2733.
23. Piepenbreier H, Sim A, Kobras CM, Radeck J, Mascher T, Gebhard S, Fritz G. 2019. From modules to networks: A systems-level analysis of the bacitracin stress response in *Bacillus subtilis*. bioRxiv doi:10.1101/827469:827469.
24. Radeck J, Gebhard S, Orchard PS, Kirchner M, Bauer S, Mascher T, Fritz G. 2016. Anatomy of the bacitracin resistance network in *Bacillus subtilis*. Mol Microbiol 100:607-20.
25. Pader V, Hakim S, Painter KL, Wigneshweraraj S, Clarke TB, Edwards AM. 2016. *Staphylococcus aureus* inactivates daptomycin by releasing membrane phospholipids. Nat Microbiol 2:16194.
26. Storm DR, Strominger JL. 1973. Complex formation between bacitracin peptides and isoprenyl pyrophosphates. The specificity of lipid-peptide interactions. J Biol Chem 248:3940-5.

27. Reiners J, Lagedroste M, Ehlen K, Leusch S, Zaschke-Kriesche J, Smits SHJ. 2017. The N-terminal Region of Nisin Is Important for the BceAB-Type ABC Transporter NsrFP from *Streptococcus agalactiae* COH1. Front Microbiol 8:1643.
28. Stein T, Heinzmann S, Dusterhus S, Borchert S, Entian KD. 2005. Expression and functional analysis of the subtilin immunity genes *spaIFEG* in the subtilin-sensitive host *Bacillus subtilis* MO1099. J Bacteriol 187:822-8.
29. Okuda K, Aso Y, Nakayama J, Sonomoto K. 2008. Cooperative transport between NukFEG and NukH in immunity against the lantibiotic nukacin ISK-1 produced by *Staphylococcus warneri* ISK-1. J Bacteriol 190:356-62.
30. Greene NP, Kaplan E, Crow A, Koronakis V. 2018. Antibiotic Resistance Mediated by the MacB ABC Transporter Family: A Structural and Functional Perspective. Front Microbiol 9:950.
31. Crow A, Greene NP, Kaplan E, Koronakis V. 2017. Structure and mechanotransmission mechanism of the MacB ABC transporter superfamily. Proc Natl Acad Sci U S A 114:12572-12577.
32. Economou NJ, Cocklin S, Loll PJ. 2013. High-resolution crystal structure reveals molecular details of target recognition by bacitracin. Proc Natl Acad Sci U S A 110:14207-12.
33. Cao M, Helmann JD. 2002. Regulation of the *Bacillus subtilis bcrC* Bacitracin Resistance Gene by Two Extracytoplasmic Function σ Factors. Journal of Bacteriology 184:6123-6129.
34. Zhao H, Sun Y, Peters JM, Gross CA, Garner EC, Helmann JD. 2016. Depletion of Undecaprenyl Pyrophosphate Phosphatases Disrupts Cell Envelope Biogenesis in *Bacillus subtilis*. J Bacteriol 198:2925-2935.
35. Radeck J, Lautenschlager N, Mascher T. 2017. The Essential UPP Phosphatase Pair BcrC and UppP Connects Cell Wall Homeostasis during Growth and Sporulation with Cell Envelope Stress Response in *Bacillus subtilis*. Front Microbiol 8:2403.
36. Schneider T, Kruse T, Wimmer R, Wiedemann I, Sass V, Pag U, Jansen A, Nielsen AK, Mygind PH, Raventos DS, Neve S, Ravn B, Bonvin AM, De Maria L, Andersen AS, Gammelgaard LK, Sahl HG, Kristensen HH. 2010. Plectasin, a fungal defensin, targets the bacterial cell wall precursor Lipid II. Science 328:1168-72.
37. Small DM. 2003. Role of ABC transporters in secretion of cholesterol from liver into bile. Proc Natl Acad Sci U S A 100:4-6.
38. Hsu ST, Breukink E, Bierbaum G, Sahl HG, de Kruijff B, Kaptein R, van Nuland NA, Bonvin AM. 2003. NMR study of mersacidin and lipid II interaction in dodecylphosphocholine micelles. Conformational changes are a key to antimicrobial activity. J Biol Chem 278:13110-7.
39. Fujinami D, Mahin AA, Elsayed KM, Islam MR, Nagao JI, Roy U, Momin S, Zendo T, Kohda D, Sonomoto K. 2018. The lantibiotic nukacin ISK-1 exists in an equilibrium between active and inactive lipid-II binding states. Commun Biol 1:150.
40. Medeiros-Silva J, Jekhmane S, Paioni AL, Gawarecka K, Baldus M, Swiezewska E, Breukink E, Weingarth M. 2018. High-resolution NMR studies of antibiotics in cellular membranes. Nat Commun 9:3963.
41. Hiron A, Falord M, Valle J, Debarbouille M, Msadek T. 2011. Bacitracin and nisin resistance in *Staphylococcus aureus*: a novel pathway involving the BraS/BraR two-component system (SA2417/SA2418) and both the BraD/BraE and VraD/VraE ABC transporters. Mol Microbiol 81:602-22.
42. Burdett V. 1996. Tet(M)-promoted release of tetracycline from ribosomes is GTP dependent. J Bacteriol 178:3246-51.
43. Trieber CA, Burkhardt N, Nierhaus KH, Taylor DE. 1998. Ribosomal protection from tetracycline mediated by Tet(O): Tet(O) interaction with ribosomes is GTP-dependent. Biol Chem 379:847-55.
44. Connell SR, Tracz DM, Nierhaus KH, Taylor DE. 2003. Ribosomal protection proteins and their mechanism of tetracycline resistance. Antimicrob Agents Chemother 47:3675-81.

629 45. Sharkey LK, Edwards TA, O'Neill AJ. 2016. ABC-F Proteins Mediate Antibiotic Resistance
630 through Ribosomal Protection. MBio 7:e01975.
631 46. Sharkey LKR, O'Neill AJ. 2018. Antibiotic Resistance ABC-F Proteins: Bringing Target
632 Protection into the Limelight. ACS Infect Dis 4:239-246.
633 47. Wilson DN. 2016. The ABC of Ribosome-Related Antibiotic Resistance. MBio 7.
634 48. Ruiz J. 2003. Mechanisms of resistance to quinolones: target alterations, decreased
635 accumulation and DNA gyrase protection. J Antimicrob Chemother 51:1109-17.
636 49. Tran JH, Jacoby GA, Hooper DC. 2005. Interaction of the plasmid-encoded quinolone
637 resistance protein QnrA with *Escherichia coli* topoisomerase IV. Antimicrob Agents
638 Chemother 49:3050-2.
639 50. Correia S, Poeta P, Hebraud M, Capelo JL, Igrejas G. 2017. Mechanisms of quinolone action
640 and resistance: where do we stand? J Med Microbiol 66:551-559.
641 51. Gebhard S, Mascher T. 2011. Antimicrobial peptide sensing and detoxification modules:
642 unravelling the regulatory circuitry of *Staphylococcus aureus*. Mol Microbiol 81:581-7.
643 52. Schmalisch M, Maiques E, Nikolov L, Camp AH, Chevreux B, Muffler A, Rodriguez S, Perkins J,
644 Losick R. 2010. Small genes under sporulation control in the *Bacillus subtilis* genome. J
645 Bacteriol 192:5402-12.

646

FIGURE LEGENDS

Fig. 1: Antibiotic resistance and flux-sensing by BceAB. A: Schematic of the BceAB-BceRS resistance system. The transporter BceAB confers resistance against bacitracin (BAC), which acts by binding its cellular target UPP. The different debated mechanisms for resistance by BceAB are indicated by dashed arrows (see text for details). Flux-sensing communicates the transport activity of BceAB to the kinase BceS (red wave arrow), causing activation of BceR, which induces transcription from the target promotor P_{bceA}. This results in increased production of BceAB, and therefore adjusted levels of resistance. As signalling is directly proportional to BceAB activity, we can use the target promotor P_{bceA} fused to a luciferase reporter to monitor transport activity. TCS, genes encoding the two-component regulatory system BceRS; ABC, genes encoding the resistance transporter BceAB. **B:** Using luciferase activity as a proxy, BceAB activity of wild-type *B. subtilis* W168 carrying the P_{bceA}-*lux* reporter fusion (WT, SGB73) was determined following 25-35 min challenge of exponentially growing cells with sub-inhibitory concentrations of bacitracin. All data are depicted as mean ± standard deviation of at least three biological replicates. **C:** Binding reaction between free bacitracin and its cellular target UPP. The change in concentration of UPP-bacitracin complexes (UPP-BAC) through manipulation of either bacitracin or UPP concentrations is indicated by bold font and upward-facing arrows.

Fig. 2: Bacitracin is neither imported nor inactivated by BceAB. Cell suspensions of OD_{600} = 10 of *B. subtilis* W168 (WT) and an isogenic Δ*bceAB* mutant (TMB035), as well as a buffer control (No cells) were incubated with 5 µg ml^{-1} bacitracin for 30 min. The biologically active bacitracin remaining in the supernatant after incubation was quantified using a bio-assay. Data are shown as mean ± standard deviation of at least three biological replicates. One-way ANOVA analysis did not show significant differences between samples.

672 **Fig. 3: Accumulation of UPP increases transport activity at low bacitracin concentrations, but does**
673 **not affect activity on lipid II binding AMPs. A, B:** Pool levels of lipid II cycle intermediates, as
674 predicted by mathematical modelling, are indicated by the relative size of blue bubbles, and
675 numbers of molecules per cell for each intermediate are given. The rate of peptidoglycan (PG)
676 synthesis is shown in molecules of precursor incorporated per minute. The thickness of the arrow for
677 *de novo* UPP synthesis reflects the previously described homeostatic increase in lipid carrier
678 synthesis upon *bcrC* deletion (23). A, wild type; B, *bcrC* deletion mutant. **C, D, E, F:** Effect of UPP
679 accumulation on transport activity *in vivo*. As a proxy for transport, luminescence activities of P_{bceA}-
680 *lux* (C, D, E) or P_{psdA}-*lux* (F) reporter strains were determined 25-35 min following challenge of
681 exponentially growing cells with varying concentrations of AMPs as indicated. Each panel shows the
682 results for one AMP given below the x-axis. Dark bars show results in the wild-type background
683 (SGB73 or SGB74), lighter bars in the isogenic Δ*bcrC* background (SGB649 or SGB681). Data are
684 shown as mean ± standard deviation of at least three biological replicates. The increased activity
685 seen in the Δ*bcrC* background compared to wild type was tested for statistical significance using
686 two-sided t-tests with *post-hoc* Bonferroni-Dunn correction for multiple comparisons (****: $p <$
687 0.0001, ***: $p < 0.001$, **: $p < 0.01$, *: $0.01 < p < 0.05$).

688

689 **Fig. 4: Depletion of UPP has a global negative effect on transport. A, B:** Pool levels of lipid II cycle
690 intermediates, as predicted by mathematical modelling, are indicated by the relative size of blue
691 bubbles, and numbers of molecules per cell for each intermediate are given. The rate of
692 peptidoglycan (PG) synthesis is shown in molecules of precursor incorporated per minute. A, wild
693 type; B, BcrC overproduction strain. **C, D, E, F:** Effect of UPP depletion on transport activity *in vivo*. As
694 a proxy for transport, luminescence activities of P_{bceA}-*lux* (C, D, E) or P_{psdA}-*lux* (F) reporter strains
695 were determined 25-35 min following challenge of exponentially growing cells with varying
696 concentrations of AMPs as indicated. Each panel shows the results for one AMP given below the x-

697 axis. Dark bars show results in the wild-type background (SGB73 or SGB74), lighter bars in a strain
698 overproducing BcrC (SGB758 or SGB974). Data are shown as mean ± standard deviation of at least
699 three biological replicates. Tests for statistical significance of differences in activity in the
700 overproduction versus wild-type backgrounds were done by two-sided t-test with *post-hoc*
701 Bonferroni-Dunn correction for multiple comparisons (****: $p < 0.0001$, ***: $p < 0.001$, **: $p < 0.01$,
702 *: $0.01 < p < 0.05$).

703

704 **Fig. 5: Accumulation of HPP does not inhibit BceAB activity.** Transport activities, using luciferase
705 activity of the P_{bceA}-*lux* reporter as a proxy, were determined for the WT (SGB927, dark grey) and a
706 HPP accumulation strain (Δ*ytpB* Δ*menA amyE*::$P_{spac(hy)}$-*menA*, SGB929, light grey) grown in MCSE
707 minimal medium, 25-35 minutes following exposure to varying bacitracin concentrations. Data are
708 shown as mean ± standard deviation of at least three biological replicates. Two-sided t-tests with
709 *post-hoc* Bonferroni-Dunn correction for multiple comparisons did not show any significant
710 difference between the wild-type and the HPP accumulation strain.

711

712 **Fig. S1: Bacitracin dose response behaviour of BceAB. A, C:** Bacitracin dose response curves of
713 BceAB activity were fitted on normalised data of the WT (SGB73) and Δ*bcrC* mutant (A, SGB649), or
714 BcrC overproduction strain (C, SGB758). To obtain the best fit of experimental data a non-linear fit
715 with variable slope was chosen. Statistical analyses of the log(EC_{50}) values using the in-build non-
716 linear regression comparison of GraphPad Prism7 showed a significant difference between the WT
717 and Δ*bcrC* mutant (****: $p < 0.0001$), but no difference between WT and BcrC overproduction strain
718 ($p = 0.73$). **B:** BceAB activity was tested in wild-type (SGB218) and Δ*bcrC* strains (SGB677), in which
719 BceAB production was uncoupled from its native regulation. Expression of *bceAB* was induced by
720 addition of 0.2 % (w/v) xylose. All data are shown as mean ± standard deviation of at least three
721 biological replicates.

TABLES

Table 1: Plasmids and bacterial strains used in this study.

Name	Genotype and description[a]	Source
Plasmids		
pAH328	Vector for transcriptional promoter fusions to *luxABCDE*; integrates in *B. subtilis sacA*; Amp^r, Cm^r	(52)
pBS2E	Empty vector; integrates in *B. subtilis lacA*; Amp^r, mls^r	(16)
pBS3Elux	Vector for transcriptional promoter fusions to *luxABCDE*; integrates in *B. subtilis sacA*; Amp^r, Mls^r	(18)
pSB1A3	Empty BioBrick standard cloning vector for *E. coli*; Amp^r	Registry of Standard Biological Parts
pSDlux101	pAH328 harbouring a transcriptional P_{bceA}-*luxABCDE* fusion	(17)
pSDlux102	pAH328 harbouring a transcriptional P_{psdA}-*luxABCDE* fusion	This study
pJNESB101	pSB1A3 harbouring *B. subtilis bcrC* in BioBrick format	This study
pJNE2E01	pBS2E harbouring a transcriptional P_{xylA}-*bcrC* fusion assembled according to the BioBrick RFC25 cloning standard	This study
pNT2E01	pBS2E harbouring P_{xylA}-*bceAB* assembled according to the BioBrick RFC10 cloning standard	(9)
pMG3Elux1	pBS3Elux harbouring a transcriptional P_{bceA}-*luxABCDE* fusion	This study
***B. subtilis* strains**		
W168	Wild type, *trpC2*	Laboratory stock
TMB035 (Δ*bceAB)*	W168 *bceAB*::kan; Kan^r	(7)
TMB297 (Δ*bcrC*)	W168 *bcrC*::tet; Tet^r	(7)
TMB713 (Δ*bceAB* Δ*bcrC*)	W168 *bceAB*::kan *bcrC*::tet; Kan^r, Tet^r	(24)
HB13350	W168 *ytpB*::spec; $Spec^r$	(14)
HB13438	W168 *menA*::kan *amyE*::$P_{spac(hy)}$-*menA;* Kan^r, Cm^r	(14)
SGB73	W168 *sacA*::pSDlux101; Cm^r	(9)
SGB74	W168 *sacA*::pSDlux102; Cm^r	This study
SGB218	W168 *bceAB*::kan *sacA*::pSDlux101 *lacA*::pNT2E01; Kan^r, Cm^r, Mls^r	(9)
SGB243	W168 *lacA*::pJNE2E01; Mls^r	This study
SGB649	W168 *bcrC*::tet *sacA*::pSDlux101; Tet^r, Cm^r	This study
SGB677	W168 *bceAB*::kan *bcrC*::*tet sacA*::pSDlux101 *lacA*::pNT2E01; Kan^r, Tet^r, Cm^r, Mls^r	This study
SGB681	W168 *bcrC*::tet *sacA*::pSDlux102; Tet^r, Cm^r	This study
SGB758	W168 *sacA*::pSDlux101 *lacA*::pJNE2E01; Cm^r, Mls^r	This study
SGB873	W168 *menA*::kan *amyE*::$P_{spac(hy)}$-*menA ytpB*:: spec; Kan^r, Cm^r, $Spec^r$	This study
SGB927	W168 sacA::pMG3Elux1; Mls^r	This study
SGB929	W168 *menA*::kan *amyE*::$P_{spac(hy)}$-*menA ytpB*:: spec *sacA*::pMG3Elux1; Kan^r, Cm^r, $Spec^r$, Mls^r	This study

SGB974	W168 *sacA*::pSDlux102 *lacA*::pJNE2E01; Cm^r, Mls^r	This study

[a] Amp^r, ampicillin resistance; Cm^r, chloramphenicol resistance; Kan^r, kanamycin resistance; Mls^r, macrolide, lincosamide and streptogramin B resistance; Tet^r, tetracycline resistance, Spec^r, spectinomycin resistance

Table 2: Primers used in this study.

Name	Description/use	Primer sequences (5'-3' direction) [a]	Source
SG0148	*lacA* insertion fwd	GCATACCGGTTGCCGTCATC	This study
SG0149	*lacA* insertion rev	GAACTACATGCACTCCACAC	This study
SG0506	*amyE* insertion fwd	GTAAGCGTTAACAAAATTCTC	This study
SG0507	*amyE* insertion rev	TTATATTGTGCAACACTTCACA	This study
SG0528	*sacA* insertion up fwd	CTGATTGGCATGGCGATTGC	(16)
SG0529	*sacA* insertion up rev	ACAGCTCCAGATCCTCTACG	(16)
SG0530	*sacA* insertion down fwd	GTCGCTACCATTACCAGTTG	(16)
SG0531	*sacA* insertion down rev	TCCAAACATTCCGGTGTTATC	(16)
SG0630	*ytpB* up fwd	TCATGTGGACCTGGAAAGCA	(14)
SG0633	*ytpB* do rev	TGATCGTCCACCGCATTACA	(14)
SG0637	*menA* up fwd	CCGTACACAAGGATAGGAGA	(14)
SG0640	*menA* do rev	GAAGGCGAAAGCATCTGACA	(14)
SG0842	P_{bceA} fwd EcoRI	CAC**GAATTC**GAACATGTCATAAGCG TGTGACG	This study
SG0883	P_{bceA} rev PstI	CGGA**CTGCAG**TATCGATGCCCTTCA GCACTTCC	This study
TM0599	P_{psdA} fwd EcoRI	AGTC**GAATTC**CACCCTCGTGAATGT GACAGC	This study
TM2242	P_{psdA} rev NotI	AATT**GCGGCCGC**CGATAGGTTCGTT GTTTGCAACACG	This study
TM2731	*bcrC* Biobrick fwd	GATC**GAATTC**GCGGCCGCT**TCTAGA** AAGGAGGTG**GCCGGC**TTGAACTAC GAAATTTTTAAAGCAATC	This study
TM2732	*bcrC* Biobrick rev	GATC**ACTAGT**ATTA**ACCGGT**GAAAT TTTGATCGGTTGGTTTTTTC	This study

[a] Sequences in bold highlight restriction sites used for cloning.

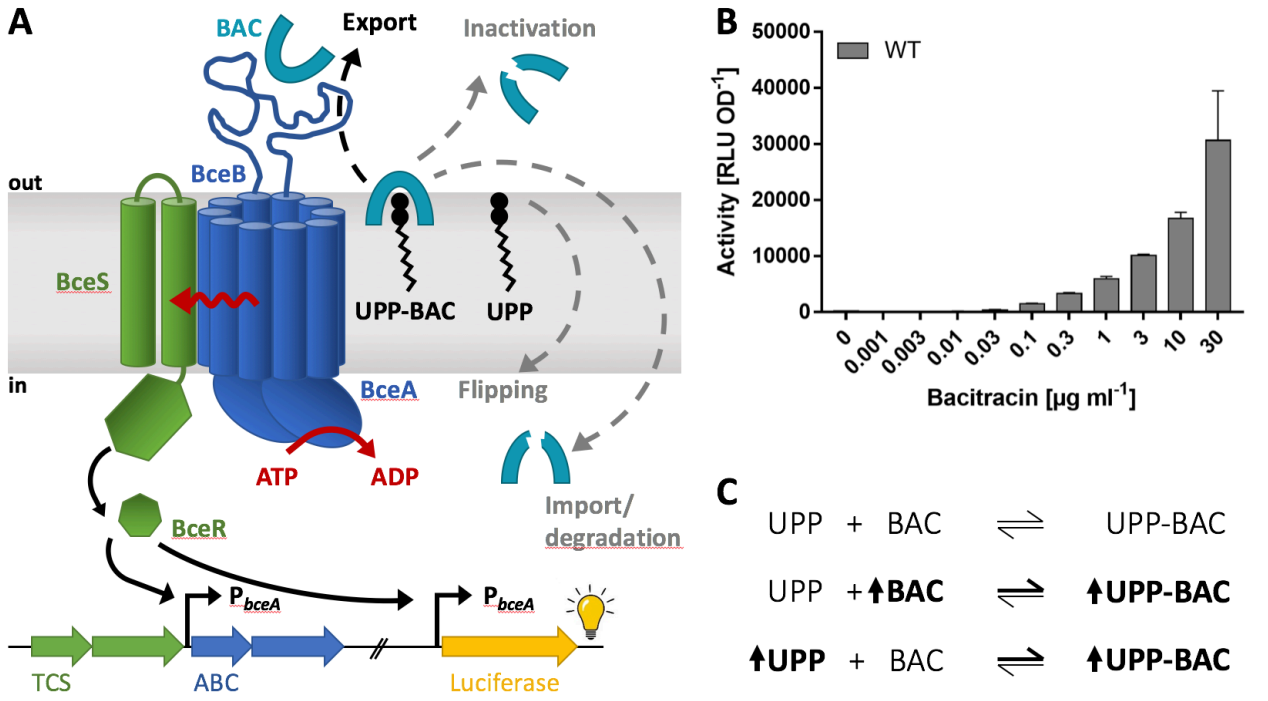

Fig. 1: Antibiotic resistance and flux-sensing by BceAB. A: Schematic of the BceAB-BceRS resistance system. The transporter BceAB confers resistance against bacitracin (BAC), which acts by binding its cellular target UPP. The different debated mechanisms for resistance by BceAB are indicated by dashed arrows (see text for details). Flux-sensing communicates the transport activity of BceAB to the kinase BceS (red wave arrow), causing activation of BceR, which induces transcription from the target promotor P_{bceA}. This results in increased production of BceAB, and therefore adjusted levels of resistance. As signalling is directly proportional to BceAB activity, we can use the target promotor P_{bceA} fused to a luciferase reporter to monitor transport activity. TCS, genes encoding the two-component regulatory system BceRS; ABC, genes encoding the resistance transporter BceAB. **B:** Using luciferase activity as a proxy, BceAB activity of wild-type *B. subtilis* W168 carrying the P_{bceA}-*lux* reporter fusion (WT, SGB73) was determined following 25-35 min challenge of exponentially growing cells with sub-inhibitory concentrations of bacitracin. All data are depicted as mean ± standard deviation of at least three biological replicates. **C:** Binding reaction between free bacitracin and its cellular target UPP. The change in concentration of UPP-bacitracin complexes (UPP-BAC) through manipulation of either bacitracin or UPP concentrations is indicated by bold font and upward-facing arrows.

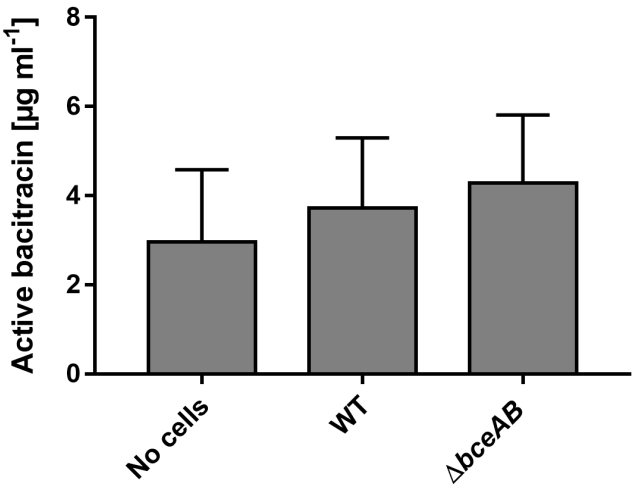

Fig.2: Bacitracin is neither imported nor inactivated by BceAB. Cell suspensions of OD_{600} = 10 of *B. subtilis* W168 (WT) and an isogenic Δ*bceAB* mutant (TMB035), as well as a buffer control (No cells) were incubated with 5 µg ml^{-1} bacitracin for 30 min. The biologically active bacitracin remaining in the supernatant after incubation was quantified using a bio-assay. Data are shown as mean ± standard deviation of at least three biological replicates. One-way ANOVA analysis did not show significant differences between samples.

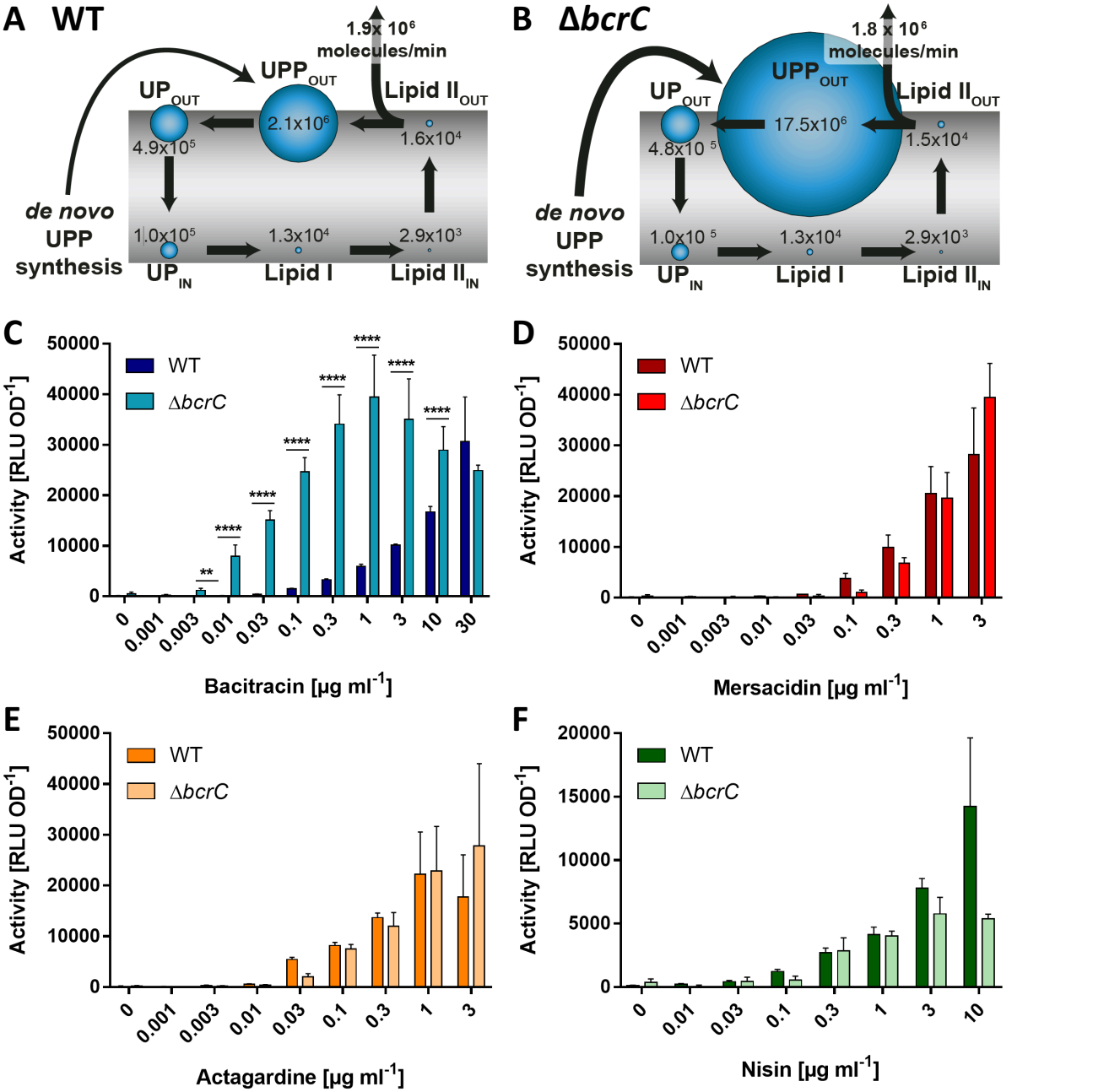

Fig. 3: Accumulation of UPP increases transport activity at low bacitracin concentrations, but does not affect activity on lipid II binding AMPs. A, B: Pool levels of lipid II cycle intermediates, as predicted by mathematical modelling, are indicated by the relative size of blue bubbles, and numbers of molecules per cell for each intermediate are given. The rate of peptidoglycan (PG) synthesis is shown in molecules of precursor incorporated per minute. The thickness of the arrow for *de novo* UPP synthesis reflects the previously described homeostatic increase in lipid carrier synthesis upon bcrC deletion (23). A, wild type; B, *bcrC* deletion mutant. **C, D, E, F:** Effect of UPP accumulation on transport activity *in vivo*. As a proxy for transport, luminescence activities of P_{bceA}-*lux* (C, D, E) or P_{psdA}-*lux* (F) reporter strains were determined 25-35 min following challenge of exponentially growing cells with varying concentrations of AMPs as indicated. Each panel shows the results for one AMP given below the x-axis. Dark bars show results in the wild-type background (SGB73 or SGB74), lighter bars in the isogenic Δ*bcrC* background (SGB649 or SGB681). Data are shown as mean ± standard deviation of at least three biological replicates. The increased activity seen in the Δ*bcrC* background compared to wild type was tested for statistical significance using two-sided t-tests with *post-hoc* Bonferroni-Dunn correction for multiple comparisons (****: $p < 0.0001$, ***: $p < 0.001$, **: $p < 0.01$, *: $0.01 < p < 0.05$).

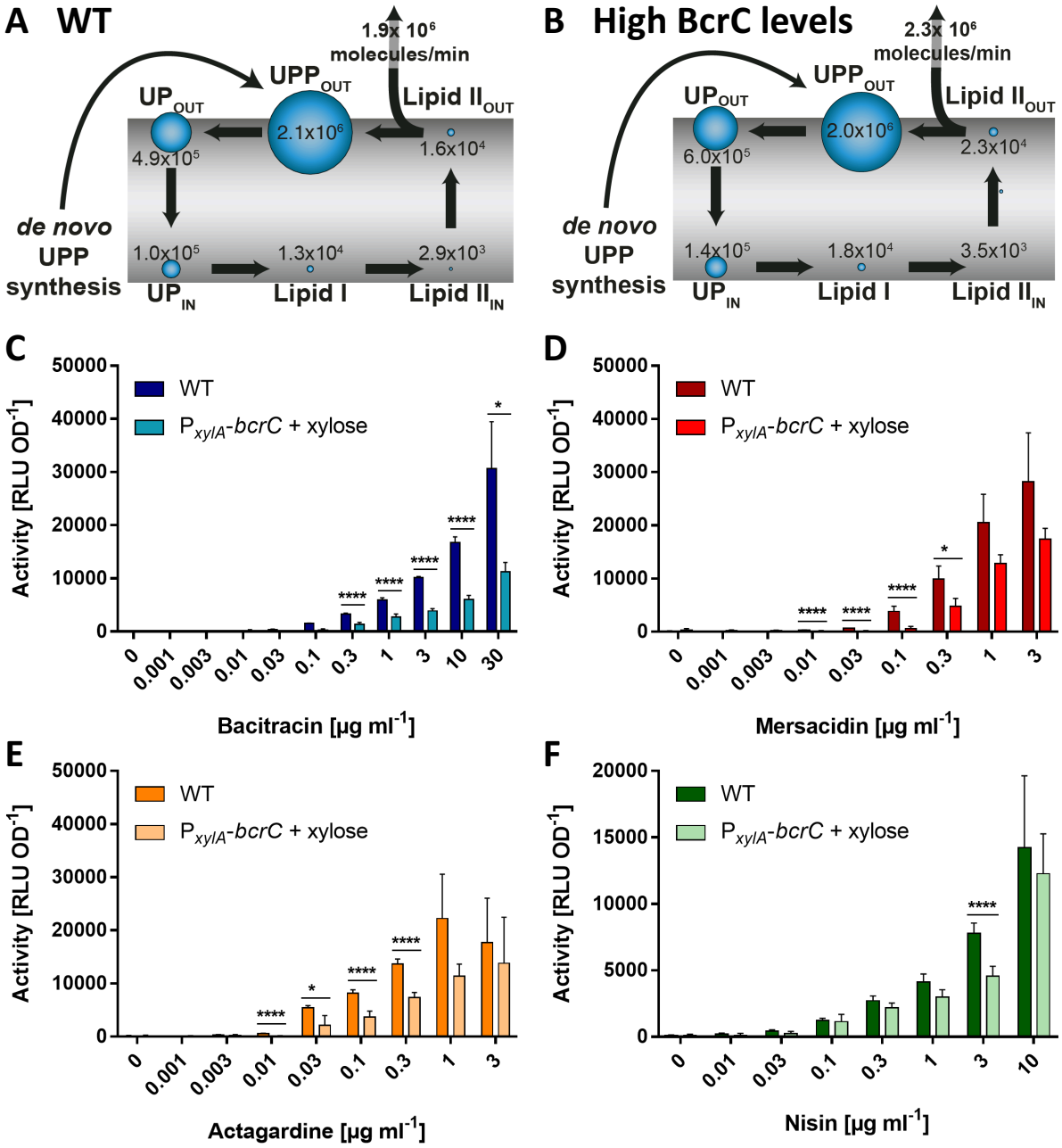

Fig. 4: Depletion of UPP has a global negative effect on transport. A, B: Pool levels of lipid II cycle intermediates, as predicted by mathematical modelling, are indicated by the relative size of blue bubbles, and numbers of molecules per cell for each intermediate are given. The rate of peptidoglycan (PG) synthesis is shown in molecules of precursor incorporated per minute. A, wild type; B, BcrC overproduction strain. **C, D, E, F:** Effect of UPP depletion on transport activity *in vivo*. As a proxy for transport, luminescence activities of P_{bceA}-*lux* (C, D, E) or P_{psdA}-*lux* (F) reporter strains were determined 25-35 min following challenge of exponentially growing cells with varying concentrations of AMPs as indicated. Each panel shows the results for one AMP given below the x-axis. Dark bars show results in the wild-type background (SGB73 or SGB74), lighter bars in a strain overproducing BcrC (SGB758 or SGB974). Data are shown as mean ± standard deviation of at least three biological replicates. Tests for statistical significance of differences in activity in the overproduction versus wild-type backgrounds were done by two-sided t-test with *post-hoc* Bonferroni-Dunn correction for multiple comparisons (****: $p < 0.0001$, ***: $p < 0.001$, **: $p < 0.01$, *: $0.01 < p < 0.05$).

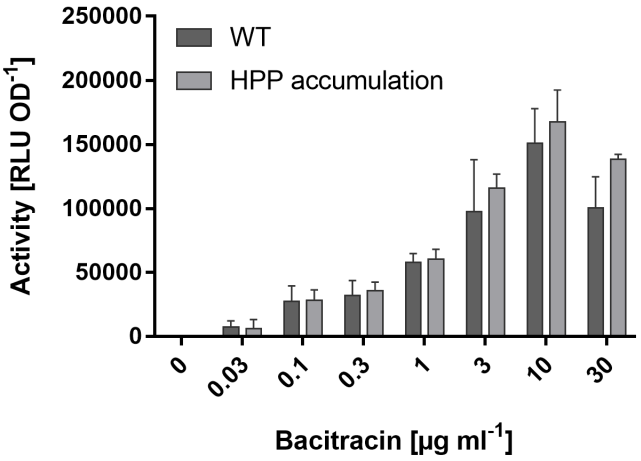

Fig. 5: Accumulation of HPP does not inhibit BceAB activity. Transport activities, using luciferase activity of the P_{bceA}-*lux* reporter as a proxy, were determined for the WT (SGB927, dark grey) and a HPP accumulation strain (Δ*ytpB* Δ*menA* *amyE*::$P_{spac(hy)}$-*menA*, SGB929, light grey) grown in MCSE minimal medium, 25-35 minuts following exposure to varying bacitracin concentrations. Data are shown as mean ± standard deviation of at least three biological replicates. Two-sided t-tests with *post-hoc* Bonferroni-Dunn correction for multiple comparisons did not show any significant difference between the wild-type and the HPP accumulation strain.

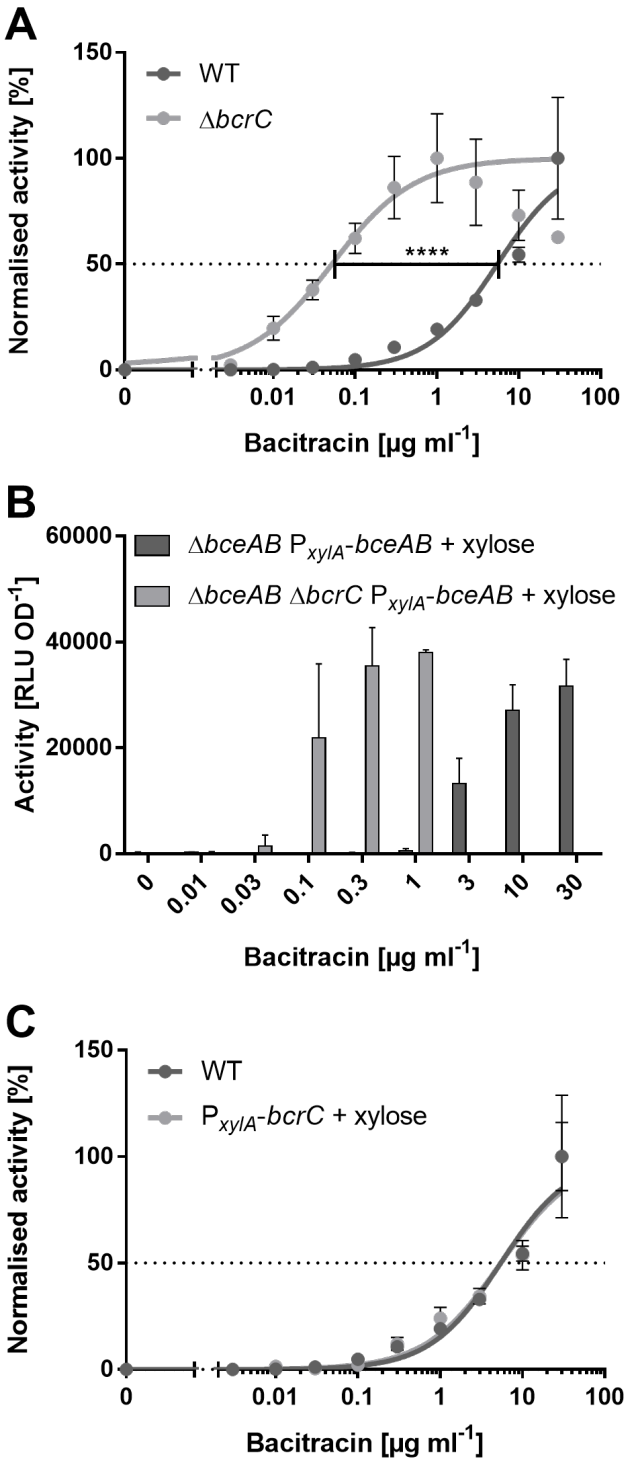

Fig. S1: Bacitracin dose response behaviour of BceAB. A&C: Bacitracin dose response curves of BceAB activity were fitted on normalised data of the WT (SGB73) and Δ*bcrC* mutant (A, SGB649), or BcrC overproduction strain (C, SGB758). To obtain the best fit of experimental data a non-linear fit with variable slope was chosen. Statistical analyses of the log(EC_{50}) values using the in-build non-linear regression comparison of GraphPad Prism7 showed a significant difference between the WT and Δ*bcrC* mutant (****: $p < 0.0001$), but no difference between WT and BcrC overproduction strain (p = 0.73). **B:** BceAB activity was tested in wild-type (SGB218) and Δ*bcrC* strains (SGB677), in which BceAB production was uncoupled from its native regulation. Expression of *bceAB* was induced by addition of 0.2 % (w/v) xylose. All data are shown as mean ± standard deviation of at least three biological replicates.